

1
2
3 **Is Weather Chaotic?**

4 **Coexistence of Chaos and Order within a Generalized Lorenz Model**

5
6 by

7
8 Bo-Wen Shen^{1,*}, Roger A. Pielke Sr.², Xubin. Zeng³, Jong-Jin Baik⁴
9 Tiffany A.L. Reyes¹, Sara Faghih-Naini^{1,5}, Robert Atlas⁶, and Jialin Cui^{1,7}

10
11 ¹Department of Mathematics and Statistics, San Diego State University, San Diego, CA, USA

12 ²CIRES, University of Colorado at Boulder, Boulder, CO, USA

13 ³Department of Hydrology and Atmospheric Science, University of Arizona, Tucson, AZ, USA

14 ⁴School of Earth and Environmental Sciences, Seoul National University, Seoul, South Korea

15 ⁵Chair for Applied Mathematics 3, Friedrich-Alexander-University Erlangen-Nuremberg,
16 Erlangen, Germany

17 ⁶AOML, National Oceanic and Atmospheric Administration, Miami, FL, USA

18 ⁷Department of Computer Sciences, San Diego State University, San Diego, CA, USA

19
20
21
22
23
24 [*bshen@sdsu.edu](mailto:bshen@sdsu.edu)

25
26
27
28
29 (To be submitted)

30 (Last Updated: 2019/09/14)

31

32 **Abstract**

33 The pioneering study of Lorenz in 1963 and a follow-up presentation in 1972 changed our
34 view on the predictability of weather by revealing the so-called butterfly effect, also known as
35 chaos. Over 50 years since Lorenz’s 1963 study, the statement of “weather is chaotic” has
36 been well accepted. Such a view turns our attention from regularity associated with Laplace’s
37 view of determinism to irregularity associated with chaos. Stated alternatively, while Lorenz
38 (1993) documented that “*as with Poincare and Birkhoff, everything centers around periodic*
39 *solutions,*” he himself and chaos advocates focused on the existence of non-periodic solutions
40 and their complexities. Now, a refined statement is suggested based on recent advances in high-
41 dimensional Lorenz models and real-world global models. In this study, we provide a report
42 to: (1) Illustrate two kinds of attractor coexistence within Lorenz models. Each kind contains
43 two of three attractors including point, chaotic, and periodic attractors corresponding to steady-
44 state, chaotic, and limit cycle solutions, respectively. (2) Suggest that the entirety of weather
45 possesses the dual nature of chaos and order associated with chaotic and non-chaotic processes,
46 respectively. Specific weather systems may appear chaotic or non-chaotic within their finite
47 lifetime. While chaotic systems contain a finite practical predictability, non-chaotic systems
48 (e.g., dissipative processes) could have better predictability (e.g., up to their lifetime). The
49 refined view on the nature of weather is neither too optimistic nor pessimistic as compared to
50 the Laplacian view of deterministic unlimited predictability and the Lorenz view of
51 deterministic chaos with finite predictability.

55

56

57

58

59

60 **Capsule**

61

62

63

64 By revealing two kinds of attractor coexistence within Lorenz models, we suggest that the

65 entirety of weather possesses a dual nature of chaos and order. The refined view on the nature

66 of weather is neither too optimistic nor pessimistic as compared to the Laplacian view of

67 deterministic predictability and the Lorenz view of deterministic chaos.

68

69

70

71 **1. Introduction**

72

73 Is weather chaotic? A view that weather is chaotic was proposed and is recognized based on
74 the pioneering work of Lorenz (1963) who first introduced the concept of deterministic chaos.
75 Defined as aperiodic solutions that display sensitive dependence on initial conditions (ICs), chaos
76 is also known as the butterfly effect. The appearance of deterministic chaos suggests finite
77 predictability, in contrast to the Laplacian view of deterministic predictability that is unlimited.
78 After a follow-up conference presentation in 1972 (Lorenz 1972), the butterfly effect has come to
79 be known as a metaphor for indicating that a tiny perturbation that is as small as a butterfly's flap
80 may generate a large impact that could create a tornado. The original Lorenz 1963 study and a
81 1972 presentation, as well as his 1969 study (Lorenz 1969), laid the foundation for chaos theory
82 that is viewed as one of the three scientific achievements of the 20th century, inspiring numerous
83 studies in multiple fields, including earth science, mathematics, philosophy, physics, etc. (Gleick
84 1987).

85

86 While the finding of a chaotic attractor has suggested a finite predictability for weather over
87 the past fifty years, such chaotic solutions indeed occur over a finite interval of time-independent
88 parameters within the Lorenz model. Therefore, other features of the original Lorenz model and
89 generalized Lorenz models that were discovered in subsequent studies (Guckenheimer and
90 Williams 1979; Sparrow 1982; Smale 1998; Tucker 2002; Musielak et al. 2005; Roy and Musielak,
91 2007; Yang and Chen 2008; Sprott et al. 2013; Moon et al. 2017, 2019; Felicio and Rech, 2018;
92 Shen 2014-2017, 2019a) should be taken into consideration in order to reveal the true nature of
93 weather. For example, in addition to chaotic solutions, other types of solutions indeed appear over
94 different intervals of parameters within the Lorenz model (Sparrow 1982), but their role in weather

95 has been overlooked. Furthermore, as emphasized by recent studies using a generalized high-
96 dimensional Lorenz model (e.g., Shen 2019a; Shen et al. 2019; Reyes and Shen 2019), two types
97 of solutions (e.g., chaotic and non-chaotic solutions) may coexist within the same model
98 parameters but for different ICs (e.g., Sprott et al. 2005; Sprott and Xiong 2015). Such a
99 coexistence indicates the possibility of a dual nature for chaos and order for weather. Thus, it is
100 important to understand whether or not and how other types of solutions and their coexistence may
101 help illustrate a more comprehensive view on the nature of weather, and improve our
102 understanding of chaotic and non-chaotic processes within different types of solutions. Stated
103 alternatively, we may ask whether the statement of “weather is chaotic” that exclusively considers
104 chaotic solutions is realistic. In this study, a specific type of solution is referred to as an
105 “attractor”, defined as the smallest attracting point set that cannot be decomposed into two or
106 more subsets with distinct regions of attraction (e.g., Sprott et al. 2013).

107

108 To address the above, here, we provide a review of major solutions using the Lorenz model
109 (LM), including three types of solutions (i.e., three attractors) and one kind of attractor coexistence.
110 We then summarize our recent findings for two kinds of attractor coexistence using a newly
111 developed, generalized, high-dimensional LM (GLM) (e.g., Shen 2019a). Based on an analysis of
112 the Lorenz model and the GLM, we suggest a refined view on the dual nature of weather.
113 Concluding remarks are provided at the end. Using a realistic value for the Prandtl number
114 (i.e., $\sigma = 1$) within the Lorenz model, Supplemental Materials are presented in order to support
115 the findings for two kinds of attractor coexistence.

116

117 **2. The Lorenz 1963 Model**

118

119 In his 1963 study, Prof. Lorenz presented an elegant system of three ordinary differential
120 equations (ODEs) using three parameters derived from the governing equations for the Rayleigh-
121 Benard convection (e.g., Saltzman 1962; Lorenz 1963). The three ODEs describe the time
122 evolution of three variables, X, Y, and Z, as follows:

123
$$\frac{dX}{d\tau} = \sigma Y - \sigma X, \quad (1)$$

124
$$\frac{dY}{d\tau} = -XZ + rX - Y, \quad (2)$$

125
$$\frac{dZ}{d\tau} = XY - bZ. \quad (3)$$

126 Here, τ is dimensionless time. The three, time-independent parameters are σ , r , and b . The first
127 two parameters represent the Prandtl number and the normalized Rayleigh number (or the heating
128 parameter), respectively. The third parameter is a function of the ratio between the vertical scale
129 of the convection cell and its horizontal scale. (X, Y, Z) represent the amplitudes of the three
130 Fourier modes for dynamic and thermodynamic variables (e.g., Table 1 of Shen 2014).
131 Specifically, X represents the amplitude of the stream function, and Y and Z represent the
132 amplitudes of the temperature deviation. Equations (1)-(3) contain three types of physical
133 processes, including buoyancy/heating, dissipative, and nonlinear processes. The linear buoyancy
134 force and the heating force are represented by σY in Eq. (1) and rX in Eq. (2), respectively. The
135 three dissipative terms are $-\sigma X$, $-Y$, and $-bZ$ and are ignored under the dissipationless condition.
136 The two nonlinear terms, $-XZ$ and XY , are derived from the nonlinear advection of the temperature
137 term within the governing equation for the Rayleigh-Benard convection (e.g., Saltzman 1962).
138 With the exception of the heating parameter (r), the following parameters are kept constant: $\sigma =$
139 10 and $b = 8/3$. A choice of $\sigma = 1$ and $b = 2/5$ is also discussed in the Supplemental Materials.

140 In additional to control runs, parallel runs with ICs that consist of control run ICs and tiny
141 perturbations ($\epsilon = 10^{-10}$) or finite perturbations ($\epsilon = -0.9$) are performed in order to reveal the
142 difference of two solutions between the control and parallel runs.

143
144 Using the state variables X, Y, and Z as coordinates, a phase space can be defined for the
145 analysis of solutions. Therefore, the dimension¹ of the phase space is equal to the number of time-
146 dependent variables or the number of ODEs. Equations (1)-(3) with three variables are referred to
147 as a three-dimensional Lorenz model (3DLM). High-dimensional LMs contain more than three
148 variables (e.g., Shen 2014). To display a solution effectively, its time varying components are
149 plotted within the phase space, which is referred to as an orbit or a trajectory.

150

151 **Lorenz’s Chaotic and Non-Chaotic Attractors**

152

153 Depending on the competitive or collective impact of nonlinear processes and linear heating
154 and dissipative processes, measured by values of the three parameters, various types of solutions
155 (i.e., different attractors) appear within the Lorenz model. Historically, the dependence of their
156 appearance on the strength of heating measured by the normalized Rayleigh parameter (r) has been
157 a focus. Steady-state, chaotic, and nonlinear oscillatory solutions have been shown to occur under
158 conditions of weak, moderate, and strong heating, respectively (e.g., Sparrow 1982; Drazin 1992;
159 Ott 2002)². The three different types of solutions are shown using $r = 20, 28,$ and $350,$ respectively,

¹ The term “dimension” is conventionally used for a system of ODEs (e.g., Hirsch et al. 2013; Thompson and Stewart 2002). In this study, the 5DLM and 7DLM are referred to as high-dimensional or high-order Lorenz models (e.g., Moon et al. 2017).

² Similar findings for the dependence of various solutions (i.e., chaotic and limit cycle solutions) on the strength of heating were also reported using a two-layer, quasi-geostrophic model that describes the finite-amplitude evolution of a single baroclinic wave by Pedlosky and Frenzen (1980).

160 in Fig. 1. The top panels display solutions for control runs within the X - Y space, while the bottom
161 panels display the time evolution of the Y components for both control and parallel runs. For a
162 steady-state solution, its orbit eventually approaches a single point, that is, a non-trivial
163 equilibrium point within the X - Y space (Fig. 1a), appearing as a point attractor; and its amplitude
164 remains constant over time after arriving at the equilibrium point. Mathematically, equilibrium
165 points, also called critical points, are defined as solutions of the time-independent nonlinear system
166 (e.g., no time derivatives in Eqs. (1)-(3), Guckenheimer and Holmes (1983))³. When the heating
167 parameter exceeds the critical value of $r_c = 24.74$, the 3DLM with $r = 28$ displays the so-called
168 chaotic solution or a chaotic attractor with irregular oscillations. The solution's boundary within
169 the X - Y space appears as a tilted "8" pattern. Interestingly, when heating becomes larger (e.g., $r =$
170 350), the system produces a nonlinear periodic solution known as a limit cycle solution or a
171 periodic attractor, as shown in Figs. 1c and 1f. Additional details on the characteristics of nonlinear
172 oscillatory solutions may be found in earlier studies (e.g., Shimizu 1979; Sparrow 1982; Strogatz
173 2015) and/or recent studies (e.g., Fig. 9 of Reyes and Shen 2019). In summary, three types of
174 attractors, including a point attractor, a chaotic attractor, and a periodic attractor (e.g., Sprott et al.
175 2013) appear and are associated with weak, moderate, and strong heating, respectively. Below, the
176 impact of a tiny initial perturbation on these attractors is further discussed.

177

178 Parallel runs with a tiny initial perturbation ($\epsilon = 10^{-10}$) are compared to control runs in order
179 to reveal the difference (also referred to as the divergence) of initial, nearby trajectories within the
180 phase space of the 3DLM. For steady-state and nonlinear oscillatory solutions, control and parallel
181 runs produce almost identical results, only appearing in red, for example, in Figs. 1d and 1f. The

³ In our 5D-, 7D-, and 9D LMs, we can obtain closed form solutions of trivial and non-trivial equilibrium points and use them to verify the numerical solutions of equilibrium points.

182 runs indicate insignificant impacts by a tiny initial perturbation. In other words, steady-state and
183 nonlinear oscillatory solutions are insensitive to a tiny change in ICs. In comparison, within the
184 chaotic regime, two solution orbits whose starting points are very close to each other display very
185 different time evolutions, as clearly shown in blue and red in Fig. 1e. The phenomenon is called
186 the sensitive dependence of solutions on ICs. As further discussed below, such a feature only
187 appears within a chaotic solution.

188

189 **Boundedness and Divergence of Chaotic Trajectories**

190

191 Within the chaotic regime of the 3DLM, a sensitive dependence of solutions on ICs is referred
192 to as the butterfly effect (BE, e.g., Lorenz 1993, 2008). As shown in Fig. 2a (e.g., as discussed on
193 page 15 of Lorenz 1993), the term “butterfly” was partly used due to its geometric pattern in the
194 Y - Z space. A butterfly pattern with a finite size and varying curvatures within the phase space also
195 qualitatively suggests an important feature of solution boundedness. Therefore, BE means that a
196 tiny change in an IC can produce a very different time evolution of a solution for three variables
197 (X , Y , Z). However, the separation (or divergence) of two orbits should be bounded by the size of
198 a butterfly pattern.

199

200 The average separation (i.e., an average divergence) of nearby trajectories has been
201 quantitatively measured using the Lyapunov exponent (LE, Wolf et al. 1985; Zeng et al. 1991,
202 1993). A positive LE suggests an exponential rate in the averaged separation of two infinitesimally
203 nearby trajectories over an infinite period of time (e.g., Eqs. (25)-(26) of Shen 2014). Chaotic
204 solutions within the 3DLM, as well as high-dimensional LMs, have a positive LE. Since the LE is

205 defined as a long-term averaged separation, researchers often misinterpret the divergence of two
206 nearby, but finitely separated, chaotic trajectories within the 3DLM as continuing over time and
207 lasting forever. The misunderstanding also makes people believe that a blow-up solution is due to
208 the divergent nature of chaos. In fact, in addition to a positive LE, solution boundedness is another
209 major feature of a chaotic system. Due to solution boundedness, a trajectory should recur within
210 the phase space (e.g., Hilborn 2000). Therefore, time-varying (local) growth rates along a chaotic
211 orbit are observed (e.g., Zeng et al. 1993) and may become negative, as indicated by a negative
212 finite time LE (e.g., Fig. 7 of Nese 1989; Fig. 1 of Eckhardt and Yao 1993; p. 397 of Ding and Li
213 2007; Fig. 3 of Bailey 2011). In other words, the infinite-time limit in the definition of an LE does
214 not imply a monotonically increasing separation between two nearby trajectories over a long
215 period of time. Two initial nearby trajectories can quickly separate and reach the bound of their
216 separation.

217

218 **Coexistence of Chaos and Order**

219

220 The 3DLM produces three different attractors and each attractor exclusively appears within
221 the phase space, depending on the interval of system parameters. The 3DLM with a single-type
222 solution suggests that either chaos or order exclusively exists. Is this realistic? Below, we present
223 a different scenario that two different attractors may coexist and dominate system dynamics in a
224 separate region (i.e., a different subspace) within the phase space, referred to as the first kind of
225 attractor coexistence. A coexistence of two different solutions, appearing within the same model,
226 and with the same parameters, but with different ICs, has been well studied using conservative
227 Hamiltonian systems (e.g., Hilborn 2000). By comparison, earlier studies within the forced

228 dissipative 3DLM (e.g., Yorke and Yorke 1979; p. 242 of Drazin 1992; p. 333 of Ott 2002) have
229 also documented the coexistence of steady-state and chaotic solutions. However, such a
230 coexistence only appears over a very small range of r , giving the length of an interval less than 0.7
231 (i.e., $24.06 < r < r_c = 24.74$). As a result, the characteristics of the coexistence and its potential role
232 in revealing the nature of weather has not been well explored.

233

234 The 3DLM with the same parameters, including $r = 24.4$, $\sigma = 10$, and $b = 8/3$, but with
235 different ICs, was used to illustrate such a coexistence in a homework problem for the course
236 entitled Computational Ordinary Differential Equations taught by the first author at San Diego
237 State University during Fall 2018. As simply shown in the animation, <https://goo.gl/scqRBo>, six
238 different orbits can clearly be categorized into two types of solutions, chaotic or steady-state.
239 Below, we apply the GLM in order to show that coexistence may appear within a wider interval
240 of the heating parameter and suggest that attractor coexistence should be considered in order to
241 refine the view of the nature of weather.

242

243 **3. The Generalized Lorenz Model**

244

245 Based on our recent studies (e.g., Shen, 2014-2019; Faghih-Naini and Shen 2018), we
246 successfully developed a GLM that: (1) is derived based on partial differential equations for the
247 Rayleigh-Benard convection⁴; (2) allows a large number of modes, say M modes, where M is an

⁴ By comparison, chaotic models in Lorenz (1996/2006, 2005) were not derived from physics-based partial differential equations.

248 odd number greater than three; and (3) produces aggregated negative feedback⁵ that is accumulated
249 from the feedback of various smaller-scale processes, yielding a larger effective dissipation in
250 higher dimensional LMs (Shen 2019a; Shen et al. 2019). As a result of aggregated negative
251 feedback, a higher-dimensional LM requires a larger critical value for the Rayleigh parameter (r_c)
252 for the onset of chaos. For example, the r_c for the 5DLM, 7DLM, and 9DLM are 42.9, 116.9, and
253 679.8, respectively, as compared to a r_c of 24.74 for the 3DLM (Shen 2019a). Fig. 2 displays
254 chaotic solutions obtained from the 3D, 5D, 7D, and 9D LMs with different heating parameters.
255 Therefore, a tiny perturbation with the same strength may play a different role within the GLM
256 with a different value of M , showing a dependence on the dimension (or the degree of spatial
257 complexity associated with a various number of modes) of the GLM.

258

259 **Two Kinds of Attractor Coexistence**

260

261 The GLM with $M = 5$ or $M = 7$ (i.e., 5DLM or 7DLM) also produces three different types of
262 solutions, including a steady-state, chaotic, and limit cycle/torus⁶. More importantly, the GLM
263 with $M = 9$ (i.e., 9DLM) displays two kinds of attractor coexistence, each with two different
264 attractors. For the first kind of coexistence, both chaotic and steady-state solutions occur
265 concurrently with the same model and the same parameters. The only difference is their ICs. Such
266 a coexistence shares properties similar to that of the 3DLM but appears over a wider range of the
267 Rayleigh parameter (e.g., $679.8 < r < 1,058$), as compared to the small interval (e.g., $24.06 < r <$

⁵ Negative feedback can be found within the so-called Lorenz-Stenflo system that extends the 3DLM with one additional ODE containing one additional mode that takes rotation into consideration (e.g., Xavier and Rech 2010; Park et al. 2015, 2016).

⁶ A torus is defined as a composite motion with two (or more) oscillatory frequencies whose ratio is irrational (e.g., Faghih-Naini and Shen, 2018).

268 24.74) for the 3DLM. In fact, since the first kind of attractor coexistence has been overlooked for
269 decades, we became aware of such a finding by Yorke and Yorke (1979) after observing
270 coexistence within the 9DLM and performing a literature review.

271

272 In addition to the first kind of attractor coexistence, the 9DLM is able to produce the second
273 kind of attractor coexistence, consisting of nonlinear, periodic (i.e., limit cycle) orbits and steady-
274 state solutions at large Rayleigh parameters (e.g., $r = 1,600$). The new kind of coexistence was
275 recently documented in Shen (2019a), Shen et al. (2019), and Reyes and Shen (2019). By
276 extending the above analysis, we now show that the 3DLM with a realistic value of $\sigma = 1$ also
277 generates two kinds of attractor coexistence, suggesting that the features are not specific to our
278 9DLM. See additional information in the Supplemental Materials.

279

280 Depending on system parameters, ICs and the dimension of the model (say the value of M
281 within the GLM), a modeling system may contain one or more attractors⁷ (e.g., a point, chaotic,
282 and/or periodic attractor) within the phase space. When both chaotic and regular attractors coexist,
283 they occupy two different regions (or two different subspaces) within the phase space. Therefore,
284 we observe two kinds of solution dependence on ICs, including (1) the dependence of solution
285 types on ICs and (2) a sensitive dependence on ICs for chaotic solutions. The former suggests that
286 an IC may lead to a chaotic or non-chaotic solution. The latter indicates that only chaotic solutions
287 display sensitive dependence on a tiny, initial perturbation. We illustrate these below.

288

289 **Two Kinds of IC Dependence and Final State Sensitivity**

⁷ The coexistence of chaotic and quasi-periodic orbits has been recently documented in a modified Lorenz system by Saiki et al. (2017).

290

291 Each of the three, single-type solutions exclusively appears. Among them, a steady-state or
292 limit cycle solution has no long-term memory regarding its ICs and initial errors. Although a
293 chaotic orbit displays the sensitivity of its time evolution to initial perturbations, its statistics (i.e.,
294 the attractor itself or the butterfly pattern within the phase space) is independent of the ICs. As
295 long as a system's parameters are given, the long-term statistics of the single-type solution is
296 already determined and is independent of ICs. In comparison, when two attractors coexist in two
297 different regions within the phase space, a different IC may lead to a different type of solution with
298 very different statistics. Thus, the impact of a tiny initial perturbation can be very different,
299 depending on its association with a chaotic or non-chaotic orbit. A tiny initial perturbation may
300 only have a short-term impact on the initial transient evolution of non-chaotic (e.g., the steady-
301 state or limit cycle) solutions or lead to a very different evolution for chaotic orbits. Below, we
302 illustrate such an impact of ICs (i.e., the location of the starting point within the phase space) on
303 determining an orbit's subsequent evolution and final destination (i.e., a point attractor or a chaotic
304 attractor).

305

306 Control runs apply three sets of ICs at different locations within the phase space: close to the
307 non-trivial equilibrium point, at the origin (i.e., a saddle point), and at point (100, 100, 100, 100,
308 100, 100, 100, 100, 100). For parallel runs, a finite-amplitude perturbation ($\epsilon = -0.9$) is added into
309 the ICs. In Fig. 3, solutions of the control runs are shown in blue, while results of parallel runs are
310 displayed in green, red, or orange. Top panels display the time evolution of Y components, while
311 bottom panels present solutions within the X-Y space. The model with $r = 680$ produces the
312 coexistence of steady-state and chaotic orbits, displaying a dependence on ICs. For the first case

313 (Figs. 3a and 3d) with the IC that is close to the non-trivial equilibrium point, the orbit moves
314 toward the equilibrium point, producing steady-state solutions. Since the orbit spirals into the non-
315 trivial equilibrium point within the X - Y space, it is also called a spiral sink solution. For the second
316 case (Figs. 3b and 3e) where an IC is close to a saddle point at the origin but away from the non-
317 trivial equilibrium point, solutions still approach the same non-trivial equilibrium point as a steady-
318 state solution, while initially displaying a different time evolution as compared to the first case.
319 On the other hand, for the third case (Figs. 3c and 3f), the model produces a chaotic solution,
320 different from the steady-state solution. A comparison between control and parallel runs suggests
321 that an initial perturbation only has a short-term impact on the initial transient evolution of steady-
322 state solutions but can lead to a very different evolution for chaotic solutions⁸. As also discussed
323 in Fig. 5 of Shen et al. (2019a), a systematic analysis of the dependence of chaotic and non-chaotic
324 orbits on ICs was previously performed using an ensemble modeling approach with 4,096
325 ensemble members.

326

327 While the appearance of stable solutions may suggest better predictability, a system with
328 coexisting solutions additionally displays final state sensitivity (e.g., Grebogi et al. 1983) when
329 ICs start near the boundary of two different attractors (i.e., solutions). As illustrated below, such a
330 final state sensitivity creates a different challenge for predictability.

331

332 **Finite and Deterministic Predictability**

333

⁸ Such a dependence on initial conditions, close to (or away from) the non-trivial equilibrium point, can be shown by the following YouTube video for a double pendulum (between 1:00-1:20): <https://www.youtube.com/watch?v=LfgA2Auyo1A>. This footnote is provided only for review.

334 The rate of a growing initial error with time has been used to determine predictability,
335 suggesting a finite predictability in chaotic (or unstable) systems. Such a growth rate is
336 proportional to the divergence of two nearby trajectories measured using a Lyapunov exponent.
337 Within the chaotic regimes of the 3DLM, as well as the GLM that contains one positive LE and
338 solution boundedness, time-varying divergence and the convergence of nearby trajectories yields
339 time-varying growth rates and, thus, time-varying predictability. Estimated predictability over a
340 short period should display a dependence on various initial states⁹. By comparison, when non-
341 chaotic (i.e., steady-state or nonlinear periodic) solutions appear as a single type of solution or
342 coexist with another type of solution, their predictability should be deterministic (unlimited). As a
343 result, when a system possesses the coexistence of chaotic and non-chaotic attractors, ICs
344 determine whether finite or deterministic predictability may appear.

345

346 **4. A Refined View on the Nature of Weather**

347

348 Since climate and weather involve open systems, an assumption of constant parameters within
349 numerical simulations using the 3DLM, as well as high-dimensional LMs, is not realistic and, thus,
350 the applicability of numerical results to realistic climate or weather should be interpreted with
351 caution. To better understand the validity of applying chaotic solutions in order to define the nature
352 of weather, below, we provide additional comments. Within the forced dissipative 3DLM, chaotic
353 solutions appear within a finite range of parameters (e.g., heating parameter), bounded on one side
354 by stable, steady-state solutions and on the other side by nonlinear periodic solutions. Chaotic
355 solutions may not be able to represent the entirety of weather. Additionally, within chaotic

⁹ As a result, we agree with Prof. Arakawa that the predictability limit is not necessarily a fixed value (Lewis 2005).

356 solutions, a tiny perturbation can always lead to a very different time evolution. Stated
357 alternatively, within the chaotic regime, the system does not have a mechanism for completely
358 removing the impact of a tiny perturbation. Although these findings are interesting, it is reasonable
359 to ask whether it is realistic to expect such an effect for any tiny perturbation (e.g., Pielke 2008).

360

361 By comparison, within the GLM with $M = 9$, or higher, that possesses coexisting chaotic and
362 steady-state solutions, a tiny initial perturbation may play a very different role. A tiny perturbation
363 may have no long-term impact when it appears to be associated with a steady-state solution,
364 suggesting that the perturbation eventually dissipates. On the other hand, a tiny perturbation may
365 lead to a large impact on the time evolution of the chaotic solution. As a result, the 9DLM with a
366 dual role for a tiny initial perturbation over a wide range of the heating parameter is more realistic
367 than the classical 3DLM. Such a comparison indicates the need to refine our view of weather by
368 taking the dual nature associated with attractor coexistence into consideration. To this end, we
369 suggest, contrary to the traditional view that weather is chaotic, that weather is, in fact, a superset
370 that consists of both chaotic and non-chaotic processes, including both order and chaos.

371

372 **Additional Support: Coexisting Solutions at Two Time Scales, Vacillation and Intransitivity**

373

374 Coexisting solutions at two time scales, which are not the same as the coexisting attractors
375 discussed above, have also been documented in scientific literature. Related studies additionally
376 support the refined view on the nature of weather. For example, co-existence of fast and slow
377 manifolds has been discussed by Lorenz (1986, 1992), Lorenz and Krishnamurthy (1987) and
378 Curry et al. (1995). Both types of solutions in Lorenz (1986) are non-chaotic. By comparison, fast

379 and slow “variables” that are chaotic may also coexist within coupled systems (e.g., Pena and
380 Kalnay 2004; Mitchell and Gottwald 2012). In fact, an analysis using a singular perturbation
381 method (Bender and Orszag 1978) indicates that the GLM also possesses the coexistence of slow
382 and fast variables that correspond to large and very small spatial modes (e.g., Eq. (2) and Eq. (4)
383 of Shen 2019a in a high-dimension phase space).

384

385 The (potential) occurrence of a nonlinear periodic solution (i.e., limit cycle) in the atmosphere
386 was first illustrated by laboratory experiments using dishpans. Based on experiments by David
387 Fultz (Fultz et al. 1959) and Raymond Hide (Hide 1953), Lorenz (1993) suggested three types of
388 solutions, including (1) steady state solutions, (2) irregular chaotic solutions, and (3) vacillation.
389 “Amplitude vacillation” is defined as a solution whose amplitude grows and periodically decays
390 in a regular cycle (Lorenz 1963c; Ghil and Childress 1987; Ghil et al. 2010). Studies by Pedlosky
391 and Smith (e.g., Pedlosky 1972; Smith 1975; Smith and Reilly 1977) found that amplitude
392 vacillation can be viewed as a limit cycle solution.

393

394 Some people may wonder whether the appearance of LCs (i.e., nonlinear periodic solutions or
395 vacillation) challenges the validity of the so-called error growth model (Lorenz 1969c, 1996;
396 Nicolis 1992; Zhang et al. 2019; i.e., a logistic equation, that has been used to analyze errors in
397 chaotic systems). Given an initial condition with a small value, the solution of the logistic equation
398 grows at an initial larger growth rate, then a nonlinear smaller growth rate, and eventually
399 approaches a constant defined as a saturated error. However, for periodic solutions such as
400 vacillation (Lorenz 1969c), the error averaged over all growing and decaying components neither
401 grows or decays. As a result, an averaged error that grows with time appears when a large number

402 of growing errors and a small number of decaying errors are averaged. From the perspective of
403 weather predictions, including a sufficiently large number of ensemble runs in order to obtain a
404 forecast score that decreases monotonically with time is often required. (Note that within the
405 logistic equation, large errors, which are larger than the value at the equilibrium point, should
406 decay nonlinearly and then linearly.) While the error model with monotonically increasing
407 solutions may describe the statistical behavior of the system within which the majority of small
408 errors tends to grow, the error model cannot accurately represent the transient evolution of the
409 specific solution consisting of decaying components or periodic solutions. In short, the decaying
410 errors that may be associated with the steady-state solutions are not explicitly included within the
411 error growth model.

412

413 In 1984, Lorenz proposed another idealized system of three ODEs for qualitatively depicting
414 atmospheric circulation, known as the Lorenz (1984) model. Since detailed derivations of the
415 Lorenz (1984) model were missing (e.g., Veen 2002a, b), it is difficult to trace the physical source
416 of the forcing terms (parameters “F” and “G” in Eqs. (1)-(3) of Lorenz 1984) in the model.
417 Additionally, as compared to fully dissipative systems where the time change rate of volume of
418 the solutions is negative, the volume of the solution within the 1984 model does not necessarily
419 shrink to zero (e.g., p. 380 of Lorenz 1990). Therefore, results obtained using the Lorenz 1984
420 model should be analyzed and interpreted with caution. Here, we illustrate some important features
421 that are consistent with our findings (e.g., Shen 2019b) that support the revised view on the dual
422 nature of weather.

423

424 Major features within the Lorenz (1984) model are summarized as follows: (1) there are three
425 types of solutions, including steady state, periodic solutions, and chaotic solutions, that depend on
426 the values of system parameters; (2) (some) periodic solutions can be identified as limit cycle
427 solutions (Wang et al., 2014); multistability with coexisting limit cycle solutions gave rise a
428 question of whether or not intransitivity may occur (i.e., whether or not any of the state solutions
429 may last forever); (3) when a seasonally varying forcing term F with a time scale of 12 months
430 was applied, chaotic solutions appear during winter and two different limit cycle solutions appear
431 during active and inactive summer, respectively (e.g., Fig. 6 of Lorenz 1990); (4) a spectral
432 analysis displays peaks at time scales of 20 days associated with solutions during the summer (e.g.,
433 Figs. 1-3 of Pielke and Zeng 1994); (5) the transition from a chaotic solution in winter to a periodic
434 solution in summer displays a final state sensitivity in association with the coexistence of two
435 different limit cycle solutions. Such a transition may be likely unpredictable. The final state
436 sensitivity suggests that the system is unlikely intransitive. However, our results indicate that
437 once summer begins and has been observed, a predictability of more than two weeks may be
438 expected during each cycle of a periodic solution during the summer months.

439

440 The above analysis supports our revised view on the dual nature of weather and the
441 hypothetical mechanism for the recurrence (or periodicity) of successive African Easterly Waves
442 (AEWs), based on the GLM, in Shen (2019b). The insensitivity of limit cycles to initial conditions
443 implies that AEW simulations could be more predictable than we assumed (i.e., a predictability of
444 more than two weeks).

445

446 **5. Concluding Remarks**

447

448 The chaotic nature of weather with finite predictability has been revealed for decades using the
449 Lorenz model (Lorenz 1963), leading to a view that weather is chaotic. By including additional
450 small-scale processes within the generalized Lorenz model (e.g., Shen 2019a), we previously
451 suggested the possibility of suppressing chaotic responses and, thus, incrementally improving
452 predictability. In this study, we further discussed coexisting attractors in order to illustrate the dual
453 nature of chaos and order in weather that leads to a different view on the intrinsic predictability of
454 weather. As a result, we suggest that the entirety of weather is a superset that consists of both
455 chaotic and non-chaotic processes. Specific weather systems may appear on a chaotic or non-
456 chaotic orbit for their finite lifetime, depending on the time scales of the energy source. The
457 refined view with a duality of chaos and order is fundamentally different from the Laplacian view
458 of deterministic predictability and the Lorenz view of deterministic chaos. The appearance of
459 periodic solutions (i.e., vacillation) and their transition to chaotic solutions associated with time
460 varying parameters were indeed documented by Prof. Lorenz using different approaches (e.g.,
461 Lorenz 1969, 1984, 1990).

462

463 The refined view is not too optimistic or too pessimistic as compared to traditional views. Both
464 potential and challenges are suggested. The refined view for a dual nature of weather permits the
465 possibility of both finite and unlimited predictability (e.g., up to the lifetime of a dissipative
466 system). Although chaotic solutions with BE have finite, time-varying predictability, as a result of
467 a sensitivity to initial conditions, they do not exclusively appear but occur within a subset of the
468 total number of solutions. By comparison, for non-chaotic processes with steady-state or nonlinear
469 periodic solutions, their intrinsic predictability is deterministic and their practical predictability

470 can be continuously increased by improving the accuracy of the model and the initial conditions.
471 To this end, if we are able to identify non-chaotic solutions such as steady-state, periodic, or quasi-
472 periodic solutions in advance, we may obtain longer predictability or better estimates on
473 predictability. Our future work will focus on developing schemes for the detection of chaotic and
474 non-chaotic solutions (e.g., Sprott and Xiong, 2015; Reyes and Shen 2019) in order to improve
475 our understanding of the roles of butterfly effects in the real world and on high-resolution global
476 models; and, thus, our understanding of the conditions under which nonlinear interactions may
477 lead to chaotic solutions and/or non-chaotic solutions such as limit cycle solutions.

478

479 **Acknowledgments:**

480 We thank reviewers of the manuscript, the editor, and Drs. R. Anthes, B. Bailey, J. Buchmann, D.
481 Durran, M. Ghil, B. Mapes, Z. Musielak, T. Krishnamurti, C.-D. Lin, J. Rosenfeld, R. Rotunno, I.
482 A. Santos, C.-L. Shie, and F. Zhang for valuable comments and discussions. We appreciate the
483 eigenvalue analysis provided by Mr. N. Ferrante. We are grateful for support from the College of
484 Science at San Diego State University.

485

486 **References**

487

488 Bailey, B., 2011: Quantifying the predictability of noisy space-time dynamical processes. *Statistics*
489 *and its Interface*, 4, 535-549.

490 Bender, C. M. and Orszag, S. A. 1978. *Advanced Mathematical Methods for Scientists and*
491 *Engineers*. McGraw-Hill, New York, pp. 593.

492 Curry, J.H., S.E. Haupt, and M.N. Limber, 1995: Truncated Systems, Initialization, and the Slow
493 Manifold, *Tellus*, 47A, 145161.

494 Ding, R. O., and J. P. Li, 2007: Nonlinear finite-time Lyapunov exponent and predictability. *Phys.*
495 *Lett.*, 354A, 396–400.

496 Drazin, P.G., 1992: *Nonlinear Systems*. Cambridge. 333pp.

497 Eckhardt, B., and D. Yao, 1993: Local Lyapunov exponents in chaotic systems. *Physica D*, 65,
498 100–108.

499 Faghih-Naini, S. and B.-W. Shen, 2018: Quasi-periodic in the Five-dimensional Non-dissipative
500 Lorenz Model: The Role of the Extended Nonlinear Feedback Loop. *International Journal of*
501 *Bifurcation and Chaos*, Vol. 28, No. 6 (2018) 1850072 (20 pages). DOI:
502 10.1142/S0218127418500724.

503 Felicio, C. C. and Rech, P. C., 2018: On the dynamics of five- and six-dimensional Lorenz models.
504 *J. Phys. Commun.* 2, 025028.

505 Fultz, D., R. R. Long, G. V. Owens, W. Bohan, R. Kaylor, and J. Weil. "Studies of Thermal
506 Convection in a Rotating Cylinder with Some Implications for Large-Scale Atmospheric
507 Motion." *Meteorol. Monographs* (American Meteorological Society) 21, no. 4 (1959).

508 Ghil, M., P. Read and L. Smith, 2010: Geophysical flows as dynamical systems: the influence of
509 Hide's experiments. in *Astronomy & Geophysics*, vol. 51, no. 4, pp. 428-435, Aug. 2010. doi:
510 10.1111/j.1468-4004.2010.51428.x

511 Ghil, M. and S. Childress, 1987: *Topics in Geophysical Fluid Dynamics: Atmospheric Dynamics,*
512 *Dynamo Theory, and Climate Dynamics*. Springer, New York, 485pp.

513 Gleick, J., 1987: *Chaos: Making a New Science*, Penguin, New York, 360 pp.

514 Grebogi, C., S. W. McDonald, E. Ott and J. A. Yorke, 1983: Final state sensitivity: An obstruction
515 to predictability. *Physics Letters A* Volume 99, Issue 9, 26 December 1983, Pages 415-418.

516 Guckenheimer, J., and Williams, R. F., 1979: Structural stability of Lorenz attractors. *Publ. Math.*
517 *IHES.* 50, 59.

518 Guckenheimer, J., and P. Holmes, 1983: *Nonlinear Oscillations, Dynamical Systems, and*
519 *Bifurcations of Vector Fields.* Springer, New York, 459pp.

520 Hide, R. "Some Experiments on Thermal Convection in a Rotating Liquid." *Quart. f. Roy.*
521 *Meteorol. Soc.* 79 (1953): 161.

522 Hilborn, R. C. 2000. *Chaos and Nonlinear Dynamics. An Introduction for Scientists and Engineers.*
523 2nd ed. Oxford University Press, New York, pp. 650.

524 Hirsch, M., S. Smale, and R. L. Devaney, 2013: *Differential Equations, Dynamical Systems, and*
525 *an Introduction to Chaos.* 3rd edition. Academic Press, 432 pp.

526 Lewis, 2005: Roots of ensemble forecasting. *Monthly weather review*, 133, 7, 1865-1885.

527 Lorenz, E., 1963: Deterministic nonperiodic flow, *J. Atmos. Sci.*, 20, 130-141.

528 Lorenz, E., 1963b: The predictability of hydrodynamic flow. *Trans. N.Y. Acad. Sci., Ser. II*, 25,
529 No. 4, 409-432.

530 Lorenz, 1963c: The mechanics of vacillation. *J. Atmos. Sci.*, 20, 448-464.

531 Lorenz, E. N., 1969a: The predictability of a flow which possesses many scales of motion. *Tellus*,
532 21, 289–307.

533 Lorenz, 1969b: Atmospheric predictability as revealed by naturally occurring analogues. *J. Atmos.*
534 *Sci.*, 26, 636-646.

535 Lorenz, E. N., 1972: Predictability: Does the flap of a butterfly's wings in Brazil set off a tornado
536 in Texas? *Proc. 139th Meeting of AAAS Section on Environmental Sciences, New Approaches*

537 to Global Weather: GARP, Cambridge, MA, AAAS, 5 pp. [Available online at
538 http://eaps4.mit.edu/research/Lorenz/Butterfly_1972.pdf.]

539 Lorenz, E.N., 1986: On the existence of a slow manifold, J. Atmos. Sci. 43, 154471557.

540 Lorenz, E. N., 1993: The Essence of Chaos. University of Washington Press, Seattle, 227pp.

541 Lorenz, E.N., 1992: The slow manifold. What is it? J. Atmos. Sci., 49, 24492451.

542 Lorenz, E. N., 1996: "[Predictability – A problem partly solved](#)" (PDF). Seminar on Predictability,
543 Vol. I, ECMWF. (also, published as Lorenz (2006))

544 Lorenz, E. N., 2005: Designing Chaotic Models. J. Atmos. Sci. 62, 1574-1587.

545 Lorenz, E. N., 2006: "[Predictability – A problem partly solved](#)". In T. Palmer & R. Hagedorn
546 (Eds.), Predictability of Weather and Climate (pp. 40-58). Cambridge: Cambridge University
547 Press. doi:10.1017/CBO9780511617652.004

548 Lorenz, E. N., 2008: The butterfly effect. Premio Felice Pietro Chisesi e Caterina Tomassoni
549 award lecture, University of Rome, Rome, April, 2008.

550 Lorenz, E.N. and V. Krishnamurthy, 1987: On the nonexistence of a slow manifold, J. Atmos. Sci.,
551 44, 29402950.

552 Mitchell L. and G. A. Gottwald, 2012: Data Assimilation in Slow–Fast Systems Using
553 Homogenized Climate Models. J. Atmos. Sci., 69, 1359-1377. DOI: 10.1175/JAS-D-11-0145.1

554 Moon, S., B.-S. Han, J. Park, J. M. Seo and J.-J. Baik, 2017: Periodicity and Chaos of High-Order
555 Lorenz Systems International Journal of Bifurcation and Chaos, Vol. 27, No. 11 (2017) 1750176
556 (11 pages) DOI: 10.1142/S0218127417501760.

557 Moon, S., J. M. Seo¹, B.-S. Ha, J. Park, and J.-J. Baik, 2019: A physically extended Lorenz
558 system. Chaos 29, 063129 (2019); <https://doi.org/10.1063/1.5095466>

559 Musielak, Z. E., Musielak, D. E. and Kennamer, K. S., 2005: The onset of chaos in nonlinear
560 dynamical systems determined with a new fractal technique, *Fractals*, 13, 19-31.

561 Nese, J. M., 1989: Quantifying Local Predictability in Phase Space. *Physica D.*, 35, 237-250.

562 Nicolis, C., 1992: Probabilistic aspects of error growth in atmospheric dynamics. *Q. J. R.*
563 *Meteorol. SOC.* (1992), 118, pp. 553-568.

564 Ott, E., 2002: *Chaos in Dynamical Systems*. 2nd Edition. Cambridge University Press. 478pp.

565 Park, J., H. Lee, Y.-L. Jeon, and J.-J. Baik, 2015: Periodicity of the Lorenz-Stenflo equations.
566 *Physica Scripta*, 90, 065201.

567 Park, J., B.-S. Han, H. Lee, Y.-L. Jeon, and J.-J. Baik, 2016: Stability and periodicity of high-order
568 Lorenz-Stenflo equations. *Physica Scripta*, 91, 065202.

569 Pedlosky, 1972: Limit cycles and unstable baroclinic waves. *J. Atmos. Sci.*, 29, 53-63.

570 Pedlosky, J. and C. Frenzen, 1980: Chaotic and Periodic Behavior of Finite-Amplitude Baroclinic
571 Waves. *J. Atmos. Sci.* 37, 1177-1196.

572 Peña, M. and Kalnay, E., 2004: Separating fast and slow modes in coupled chaotic systems,
573 *Nonlin. Processes Geophys.*, 11, 319-327, <https://doi.org/10.5194/npg-11-319-2004>, 2004.

574 Pielke, R., 2008: The real butterfly effect. [Available online at
575 <http://pielkeclimatesci.wordpress.com/2008/04/29/the-realbutterfly-effect/>.]

576 Pielke, R.A. and X. Zeng, 1994: Long-term variability of climate. *J. Atmos. Sci.*, 51, 155-159.

577 Reyes, T. and B.-W. Shen, 2019: A Recurrence Analysis of Chaotic and Non-Chaotic Solutions
578 within a Generalized Nine-Dimensional Lorenz Model. *Chaos, Solitons & Fractals*. 125 (2019),
579 1-12. <https://doi.org/10.1016/j.chaos.2019.05.003>

580 Roy, D. and Z. E. Musielak, 2007: Generalized Lorenz models and their routes to chaos. I. energy-
581 conserving vertical mode truncations, *Chaos Soliton. Fract.*, 32, 1038-1052.

582 Saiki, Y., E. Sander, and J. A. Yorke, 2017: Generalized Lorenz equations on a three-sphere. The
583 European Physical Journal Special Topics, 226, 1751-1764.

584 Saltzman, B., 1962: Finite amplitude free convection as an initial value problem, J. Atmos. Sci.,
585 19, 329-341.

586 Smith, R.K., 1975: [A note on a theory of vacillating baroclinic waves](#). J. Atmos. Sci., 32, 2027.

587 Smith, R. K. and J. M. Reilly, 1977: On a theory of amplitude vacillation in baroclinic waves:
588 Some numerical solutions. J. Atmos. Sci., 34, 1256-1260.

589 Shen, B.-W., 2019a: Aggregated Negative Feedback in a Generalized Lorenz Model.
590 International Journal of Bifurcation and Chaos, Vol. 29, No. 3 (2019) 1950037 (20 pages).
591 <https://doi.org/10.1142/S0218127419500378>

592 Shen, B.-W., 2019b: On the Predictability of 30-Day Global Mesoscale Simulations of African
593 Easterly Waves during Summer 2006: A View with the Generalized Lorenz Model. Geosciences
594 2019, 9, 281.

595 Shen, B.-W., 2018: On periodic solutions in the non-dissipative Lorenz model: the role of the
596 nonlinear feedback loop. Tellus A: 2018, 70, 1471912,
597 <https://doi.org/10.1080/16000870.2018.1471912>.

598 Shen, B.-W., 2017: On an extension of the nonlinear feedback loop in a nine-dimensional Lorenz
599 model. Chaotic Modeling and Simulation (CMSIM), 2: 147–157, 2017.

600 Shen, B.-W., 2016: Hierarchical scale dependence associated with the extension of the nonlinear
601 feedback loop in a seven-dimensional Lorenz model. Nonlin. Processes Geophys., 23, 189-203,
602 doi:10.5194/npg-23-189-2016, 2016.

603 Shen, B.-W., 2015: Nonlinear Feedback in a Six-dimensional Lorenz Model. Impact of an
604 additional heating term. *Nonlin. Processes Geophys.*, 22, 749-764, doi:10.5194/npg-22-749-
605 2015, 2015.

606 Shen, B.-W., 2014: Nonlinear Feedback in a Five-dimensional Lorenz Model. *J. of Atmos.*
607 *Sci.*, 71, 1701–1723. doi:<http://dx.doi.org/10.1175/JAS-D-13-0223.1>

608 Shen, B.-W., T. A. L Reyes and S. Faghih-Naini, 2019: Coexistence of Chaotic and Non-Chaotic
609 Orbits in a New Nine-Dimensional Lorenz Model. In: Skiadas C., Lubashevsky I. (eds) 11th
610 Chaotic Modeling and Simulation International Conference. CHAOS 2018. Springer
611 Proceedings in Complexity. Springer, Cham. https://doi.org/10.1007/978-3-030-15297-0_22

612 Shimizu, T., 1979: Analytical Form of the Simplest Limit Cycle in the Lorenz Model: *Physica*,
613 97A, 383-398.

614 Smale, S., 1998: Mathematical Problems for the Next Century. *The Mathematical Intelligencer* 20,
615 no. 2, pages 7–15.

616 Sparrow, C., 1982: *The Lorenz Equations: Bifurcations, Chaos, and Strange Attractors*. Springer,
617 New York. *Appl. Math. Sci.*, 269 pp.

618 Sprott, J. C. and A. Xiong, 2015: Classifying and Quantifying Basins of Attraction. *Chaos* 25,
619 083101 (2015). <http://dx.doi.org/10.1063/1.4927643>

620 Sprott, J. C., X. Wang and G. Chen, 2013: Coexistence of Point, periodic and Strange attractors.
621 *International Journal of Bifurcation and Chaos*, Vol. 23, No. 5.
622 DOI:10.1142/S0218127413500934.

623 Sprott, J.C., J.A. Vano, J.C. Wildenberg, M.B. Anderson, J.K. Noel, 2005: Coexistence and Chaos
624 in Complex Ecologies. *Physics Letters A* 335 (2005) 207–212.

625 Strogatz, S. H., 2015: Nonlinear Dynamics and Chaos. With Applications to Physics, Biology,
626 Chemistry, and Engineering. Westpress view, Boulder, CO, 513 pp.

627 Thompson, J. M. T. and H. B. Stewart, 2002: Nonlinear Dynamics and Chaos. 2nd edition. John
628 Wiley & Sons, LTD, 437 pp.

629 Tucker, W., 2002: A Rigorous ODE Solver and Smale's 14th Problem. Found. Comput. Math. 2,
630 53-117.

631 Veen, L. van, 2002a: Time scale interaction in low-order climate models. Utrecht University
632 Repository. (PhD Dissertation).

633 Veen, L., 2002b: "Baroclinic flow and the Lorenz-84 model," Int. J. Bifurcation Chaos, 13, 2117
634 (2003). DOI: <http://dx.doi.org/10.1142/S0218127403007904>

635 Wang, H., Y. Yu, and G. Wen, 2014: Dynamical Analysis of the Lorenz-84 Atmospheric
636 Circulation Model. Journal of Applied Mathematics Volume 2014, Article ID 296279, 15 pages.
637 <http://dx.doi.org/10.1155/2014/296279>.

638 Wolf, A., J. B. Swift, H. L. Swinney, and J. A. Vastano, 1985: Determining Lyapunov Exponents
639 from a Time Series. Physica, 16D, 285-317.

640 Xavier, J. C., and P. C. Rech, 2010: Regular and chaotic dynamics of the Lorenz-Stenflo system.
641 International Journal of Bifurcation and Chaos, 20 145-152.

642 Yang, Q. and G. Chen, 2008: A chaotic system with one saddle and two stable node-foci.
643 International Journal of Bifurcation and Chaos, Vol. 18, No. 5, 05.2008, p. 1393-1414.

644 Yorke, J. and E. Yorke, 1979: Metastable chaos: The transition to sustained chaotic behavior in
645 the Lorenz model. J. Stat. Phys. 21, 263-277.

646 Zeng, X., R. Eykholt, and R.A. Pielke, 1991: Estimating the Lyapunov-exponent spectrum from
647 short time series of low precision. Phys. Rev. Lett., 66, 3229-3232.

648 Zeng, X., R. A. Pielke Sr., and R. Eykholt, 1993: Chaos Theory and Its Applications to the
649 Atmosphere. *Bulletin of the Atmospheric Meteorological Society*. Vol. 74, No. 4, 631-644.

650 Zhang, F., Y. Q. Sun, L. Magnusson, R. Buizza, S.-J. Lin, J.-H. Chen, K. Emanuel, 2019: What
651 Is the Predictability Limit of Midlatitude Weather? *J. of Atmos.* 76, 1077-1091.

652

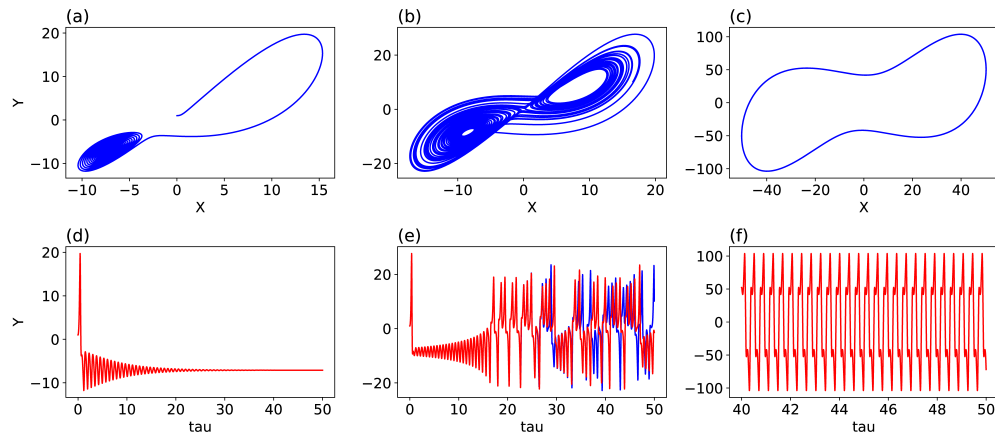
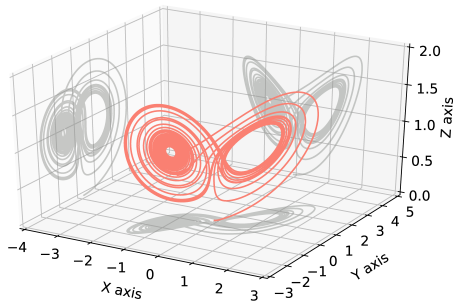
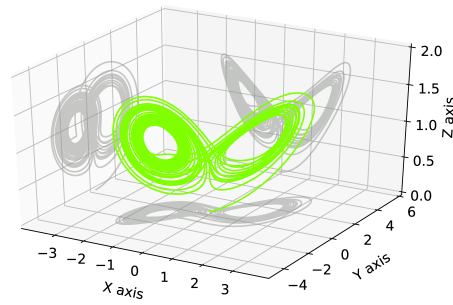


Figure 1: Three types of solutions within the 3DLM. Left, middle, and right panels display steady-state, chaotic, and limit cycle solutions at small, moderate, and large heating parameters (i.e., $r = 20, 28,$ and 350), respectively. The solutions are categorized into a point attractor, a chaotic attractor, and a periodic attractor, respectively. Top panels show orbits within the $X - Y$ space and bottom panels depict the time evolution of Y . Blue lines provide solutions from control runs. To display results from parallel runs, red lines are added in the bottom panels. Sensitive dependence on initial conditions is shown in panel (e) with two visible lines. Panels (b) and (e) are reproduced from Shen (2019b).

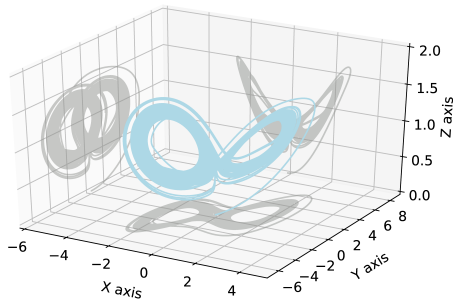
(a) $M = 3, r = 28$



(b) $M = 5, r = 45$



(c) $M = 7, r = 120$



(d) $M = 9, r = 680$

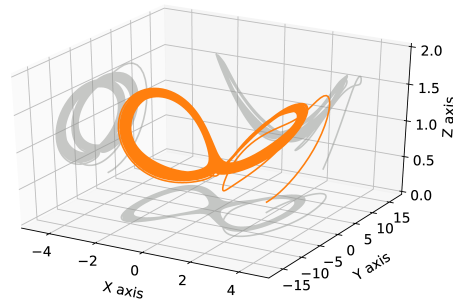


Figure 2: Chaotic solutions in the $X - Y - Z$ phase space within the 3D, 5D, 7D, and 9D Lorenz models (LMs). Panels (a)-(c) use the same initial conditions with $Y = 1$ and the remaining as zero, while panel (d) uses the IC with 100 for all variables. Variables (X, Y, Z) are normalized by $2\sqrt{r - 1}$, $2\sqrt{r - 1}$, and $(r - 1)$, respectively. A larger heating parameter is required for the onset of chaos in a higher-dimensional LM. Reproduction from Shen (2016) and Shen (2019).

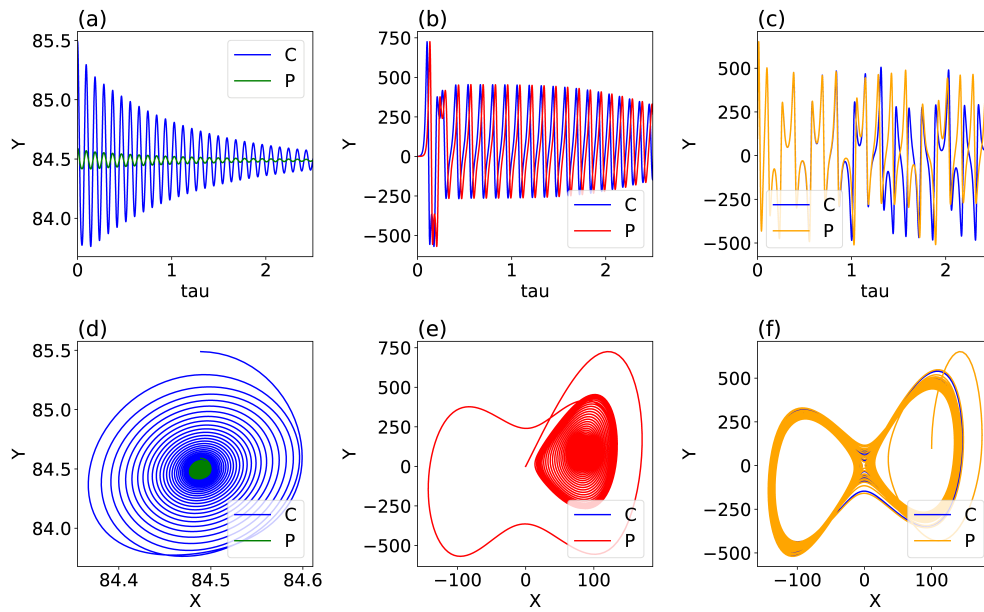


Figure 3: Solutions of the GLM with $M = 9$ and $r = 680$. Initial conditions are placed near the non-trivial critical point and the origin (i.e., trivial critical point) and at $(100, 100, 100, 100, 100, 100, 100, 100, 100)$. Top panels show the time evolution of Y for $t \in [0, 2.5]$, while bottom panels display the corresponding solutions $t \in [0, 10]$ within the $X - Y$ space. Control and parallel runs are denoted by 'C' and 'P', respectively. A finite-amplitude perturbation ($\epsilon = -0.9$) is added into the parallel runs. Panels (c) and (f) are reproduced from Shen (2019a).

653 **Supplemental Materials: Was $\sigma = 10$ a Magic Choice?**

654

655 For the past 50 years, although various types of solutions for Lorenz (1963) have been
656 documented, chaotic solutions have been a main focus. As discussed in the main text, since chaotic
657 solutions appear over a finite range of parameters, their applicability in revealing the nature of
658 weather depends on the realism of not only the models employed but also model parameter values.
659 In his book in 1993, Lorenz humbly expressed that it may not be possible for him to discover the
660 butterfly-pattern solution if a realistic value of $\sigma = 1$ was used, as shown below:

661 ``

662 *I was lucky in more ways than one. An essential constant of the model is the Prandtl number -*
663 *- the ratio of the viscosity of the fluid to the thermal conductivity. Barry had chosen the value 10.0*
664 *as having the order of magnitude of the Prandtl number of water. As a meteorologist, he might*
665 *well have chosen to model convection in air instead of water, in which case he would probably*
666 *have used the value 1.0. With this value the solutions of the three equations would have been*
667 *periodic, and I probably would never have seen any reason for extracting them from the original*
668 *seven.*

669 ‘‘

670 Therefore, one may wonder how fortunate Prof. Lorenz was and whether a realistic value of
671 $\sigma = 1$ may have influenced our view on the nature of weather. We make an attempt of addressing
672 the question by analyzing a GLM with $M = 9$ and examining a 3DLM with $\sigma = 1$. As discussed
673 in Shen (2019), the GLM with $M = 9$ has stable, non-trivial equilibrium points for all $r > 1$ when
674 $\sigma = 10$ and $b = 8/3$. To have stable, non-trivial equilibrium points for $\sigma = 1$ within the 3DLM, we
675 chose $b = 2/5$. Such a choice leads to two kinds of attractor coexistence, a unique feature first

676 identified within the 9DLM (Shen 2019). With $\sigma = 1$ in the 3DLM, the first kind of coexistence
677 includes chaotic and steady-state solutions at a moderate heating parameter (e.g., $r = 170$, as shown
678 in Fig. S1). The second kind of coexistence consists of a limit cycle and a steady-state solution at
679 a large heating parameter (e.g., $r = 250$, not shown). Table S1 lists initial conditions for the results
680 provided in Fig. S1. Thus, chaotic solutions may still appear within the 3DLM for a realistic value
681 of $\sigma = 1$, but they coexist with steady-state solutions. The appearance of chaotic solutions depends
682 not only on the range of the heating parameter but also on the ICs.

683

684 Both traditional and new model configurations with $(\sigma, b) = (10, 8/3)$ and $(1, 2/5)$,
685 respectively, can produce chaotic solutions. For the traditional configuration that has been well
686 applied in numerous studies since Lorenz (1963), all of the three equilibrium points are unstable
687 when $r > 24.74$. The stability of three equilibrium points for $\sigma = 10$, as well as for $\sigma = 1$, is
688 illustrated in Fig. S2. The non-existence of stable equilibrium points within the chaotic regime
689 makes it easier to obtain chaotic solutions. However, no tiny, initial perturbation can completely
690 lose its impact within the chaotic regime. We may interpret this as a finding that a tiny, initial
691 perturbation cannot completely dissipate (before leading to a large impact). By comparison, for
692 the new configuration, while the origin is still a saddle point, the two, non-trivial equilibrium points
693 are stable (Fig. S2b). The existence of stable equilibrium points enables the coexistence of chaotic
694 and steady-state solutions, the latter of which has no long-term memory regarding a tiny, initial
695 perturbation.

696

697 As a result of coexistence for $\sigma = 1$ within the 3DLM, a proper choice of initial conditions is
698 required in order to simulate a chaotic solution. Without knowing this, Prof. Lorenz thought that

699 it may be impossible to obtain a “strange” solution if $\sigma = 1$ was first used in the Saltzman (1962)
700 model, giving no motivation for him to work on the 3DLM. In other words, the value of $\sigma = 10$
701 used in the original study (e.g., Saltzman, 1962) was indeed a “fortunate” choice so that an
702 unexpected irregularly oscillatory solution could be revealed, inspiring Prof. Lorenz to develop
703 the 3DLM to discover the interesting chaotic features. However, on the other hand, we now
704 understand that such a configuration can only depict a partial picture for the nature of weather.
705 Based on our results and analysis, a realistic system should include physical processes for (some
706 of) the tiny disturbances in order to completely dissipate. Since it produces the coexistence of
707 chaotic and steady-state solutions and since the steady-state solution has no long-term memory of
708 tiny perturbations, the 3DLM with the new configuration of $\sigma = 1$ satisfies the objective. Such a
709 system, which is similar to the 9DLM that produces two kinds of coexisting attractors, provides a
710 more realistic view on the true nature of weather than the original 3DLM with a typical
711 configuration. The above analysis supports our refined view that weather is a superset that consists
712 of chaotic (with BE) and non-chaotic (without BE) processes.

Table S1: Initial conditions (ICs) for revealing the coexistence of two attractors for $\sigma = 1$, $b = 0.4$, and $r = 170$ within the 3DLM. $X_c = Y_c = \sqrt{b(r-1)}$ and $Z_c = (r-1)$. The six rows provide the ICs for Fig. S1.

X	Y	Z
X_c	$Y_c + 1$	Z_c
$-X_c$	$-Y_c + 1$	Z_c
0	1	0
-76.72346293	37.62433028	-146.96230812
-27.75526885	167.67883615	3.66782724
136.44623635	99.45689394	-19.76741851

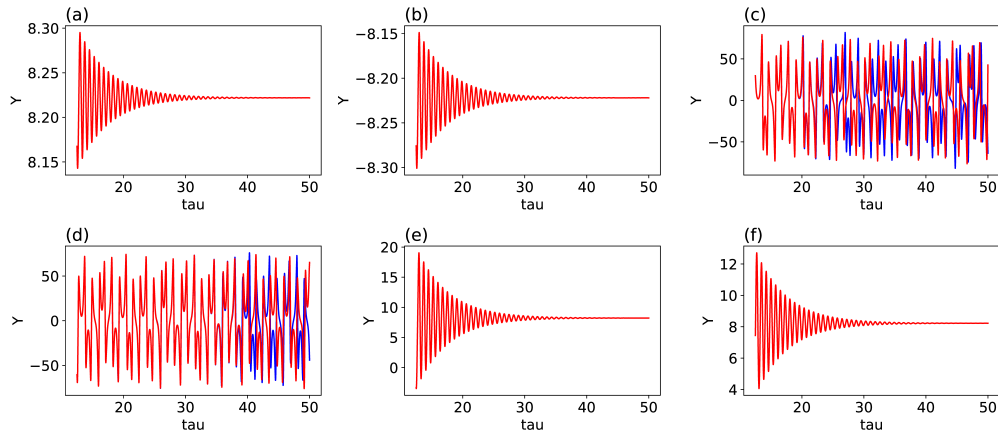
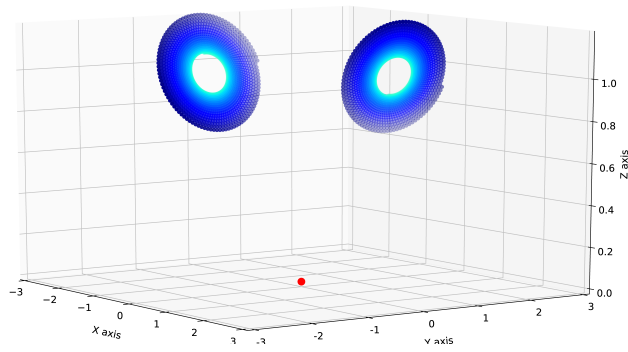


Figure S1: A co-existence of chaotic (c, d) and non-chaotic (a, b, e, f) solutions using the same parameters for $\sigma = 1$, $b = 0.4$, and $r = 170$ within the 3DLM. Blue and red lines display solutions from the control and parallel runs, respectively. Initial conditions for the results in six panels are listed in Table S1.

(a)



(b)

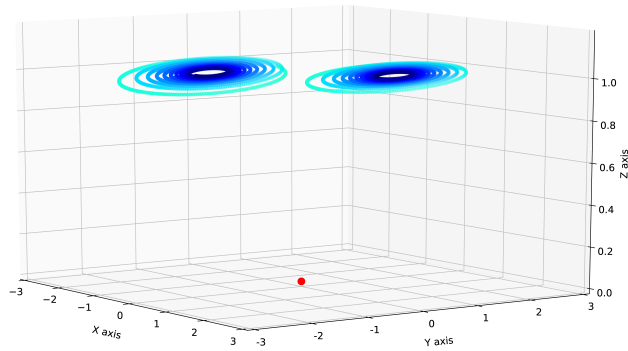


Figure S2: Local behavior near the two non-trivial critical points for the 3DLM with $\sigma = 10$ (a) and $\sigma = 1$ (b). Lighter blue dots indicate the locations of orbits at earlier times. A red dot indicates the origin, which is a saddle point. Orbits in panel (a) spiral away from the non-trivial critical points while orbits in panel (b) spiral toward the non-trivial critical points.